Nano-scale solid-phase isobaric labeling for multiplexed quantitative phosphoproteomics

Kosuke Ogata[1], Chia-Feng Tsai[1], Yasushi Ishihama*[1,2]

1) Department of Molecular & Cellular BioAnalysis, Graduate School of Pharmaceutical Sciences, Kyoto University, Kyoto 606–8501, Japan

2) Laboratory of Clinical and Analytical Chemistry, National Institute of Biomedical Innovation, Health and Nutrition, Ibaraki, Osaka, 567-0085, Japan.

*Corresponding author:
Tel: +81-75-753-4555, Fax: +81-75-753-4601, E-mail: yishiham@pharm.kyoto-u.ac.jp

ABSTRACT

We established a workflow for highly sensitive multiplexed quantitative phosphoproteomics using a nano-scale solid-phase tandem mass tag (TMT) labeling reactor. Phosphopeptides were firstly enriched by titanium oxide chromatography and then labeled with isobaric TMT reagents in a StageTip packed with hydrophobic polymer-based sorbents. We found that TMT-labeled singly phosphorylated peptides tend to flow through the titanium oxide column. Therefore, TMT labeling should be performed after the enrichment step from tryptic peptides, resulting in the need for micro-scale reaction with small amounts of phosphopeptides. Using an optimized protocol for tens to hundreds of nanograms of phosphopeptides, we obtained a nearly 10-fold increase in sensitivity compared to the conventional solution-based TMT protocol. We demonstrate that this nano-scale phosphoproteomics protocol works for 50 μg of HeLa proteins treated with selumetinib, and we successfully quantified the selumetinib-regulated phosphorylated sites on a proteome scale. The MS raw data files have been deposited with the ProteomeXchange Consortium via the jPOST partner repository (http://jpostdb.org) with the data set identifier PXD025536.

Keywords: TMT labeling, solid-phase reactor, phosphopeptides, titanium oxide chromatography, multiplexed phosphoproteomics

INTRODUCTION

Protein phosphorylation is well known as a pivotal factor in intracellular signal transduction pathways that regulate various cell functions, such as cell growth, metabolism, and apoptosis.[1,2] Therefore, in-depth analysis of the entire phosphoproteome of interest is indispensable to clarify the dynamics of complex cellular signaling networks, as well as to understand disease mechanisms and the modes of action of drugs. Recent advances in mass spectrometry (MS)-based phosphoproteomics have made it possible to identify tens of thousands of phosphopeptides from complex biological samples. This is due to the improved dynamic range, scan speed, and sensitivity in MS,[3–6] as well as the improved performance of LC with the use of columns packed with sub-2 micron silica particles,[7–9] monolithic silica columns,[10–12] and pillar array columns[13,14] for high-resolution separations. The ability to enrich phosphopeptides by metal affinity chromatography using immobilized metal ions or metal oxide particles has also made a significant contribution.[15–19]

Quantitative proteomics via isobaric chemical tags such as tandem mass tag (TMT) is attractive due to its sample multiplexing capability, high precision, and high throughput.[20] Isobaric labeling approaches enable parallel quantitation through monitoring the reporter product ions generated from the isobaric precursor ions of multiplexed samples. Although the quantitative accuracy was low in early studies because of the co-isolation of non-targeted precursor ions, this issue has been solved via several approaches, such as the introduction of MS^3 scan[21,22] in combination with a real-time search strategy[23], and/or ion mobility spectrometry.[24–26] Another advantage of isobaric labeling is that multiplexing samples provides increased sensitivity for precursor and product ions, including peptide sequence information. Furthermore, the detection sensitivity of peptides from a small amount of sample can be improved by using a carrier sample containing sufficient amounts of the target peptides.[27,28] However, the spiking amount of carrier peptides should be determined after consideration of the dynamic range of the instrument,[29] and care should be taken in handling small amounts of samples before the isobaric labeling reaction.

In multiplexed quantitative phosphoproteomics studies using TMT reagents, the labeling reaction is often performed before phosphopeptide enrichment in order to reduce the technical variation between samples.[30,31] However, peptide modification with TMT changes the chemical properties, and, in our experience, causes selectivity changes in TiO_2 chromatography for phosphopeptide enrichment. In fact, two papers have reported low recovery of TMT-labeled phosphopeptides in TiO_2 chromatography.[32,33] However, the reasons for the low recovery have not been established yet. In addition, this strategy needs relatively large amounts of the expensive TMT reagents for unphosphorylated peptides, since the content of phosphopeptides is generally less than 1% in the digest of mammalian proteomics samples.

Even with an optimized TMT labeling protocol that reduces the amount of TMT reagents used, large-scale phosphoproteomics experiments can be very costly.[34] On the other hand, enrichment of phosphopeptides followed by TMT labeling reduces the amount of TMT reagent needed, but requires highly reproducible steps for both phosphopeptide enrichment and TMT labeling.[35,36] When the starting sample is small (less than 100 µg), the amount of enriched phosphopeptides will be on the sub-microgram scale, and it is difficult to label such small amounts of peptide with TMT using standard in-solution-based protocols. It has been reported that solid-phase TMT labeling of peptides using a reversed-phase solid-phase extraction (SPE) column is more sensitive than conventional solution-phase TMT labeling.[37–40] With careful optimization, 1-2 µg of peptides can be labeled with TMT on the solid phase,[38,39] but the applicability of such micro-scale solid-phase labeling to phosphopeptides has not been evaluated yet.

Here we systematically evaluated the influence of TMT modification on phosphopeptide enrichment by TiO_2 chromatography. We established a reproducible and sensitive phosphoproteomics workflow in which the TMT labeling reaction is conducted after the phosphopeptide enrichment step, by utilizing a StageTip-based solid-phase reactor. The reaction pH, reversed-phase sorbent, and ion-pairing reagent were all found to be critical for the successful labeling of phosphopeptides. As a benchmark experiment, we profiled phosphoproteomic changes of HeLa cells in response to MKK1/2 inhibitor (selumetinib) treatment. About 10,000 unique phosphopeptides were quantified from 50 µg aliquots of starting material in triplicate analyses.

EXPERIMENTAL SECTION

Materials.

Titanium dioxide (TiO_2, titania) particles (Titansphere, particle size: 10 µm), Empore SDB-XC, C18 and C8 membrane disks, InertSep RP-C18, InertSep PLS-2, and InertSep RP-1 particles were obtained from GL Sciences (Tokyo, Japan). Sep-Pak tC18 and Oasis HLB beads were purchased from Waters (Milford, MA). Sequencing-grade modified trypsin was purchased from Promega (Madison, WI). Selumetinib was purchased from Selleck Chemicals (Houston, TX). MS-grade Lys-C (lysyl endopeptidase), DL-lactic acid, and all other chemicals were purchased from Fujifilm Wako (Osaka, Japan). Water was purified by a Millipore Milli-Q system (Bedford, MA).

Preparation of HeLa Cells.

HeLa cells were cultured to 80% confluence in DMEM containing 10% FBS in 15 cm diameter dishes. Cells were washed twice with ice-cold PBS, collected using a cell scraper, and pelleted by centrifugation. For selumetinib treatment, the medium was changed to DMEM containing 0.1% FBS after the cells had reached 80% confluence, then after incubation for 24 h, the cells were treated with selumetinib (10 μM) or vehicle DMSO for 30 min, followed by EGF (150 ng/mL) stimulation for 15 min.

The proteins were extracted as described previously.[41] In short, the cell pellets were suspended in 1 mL of buffer (12 mM sodium deoxycholate, 12 mM sodium lauroyl sarcosinate in 100 mM Tris-HCl, pH 9.0), containing protein phosphatase inhibitor cocktail 1 and 2 (Sigma) and protease inhibitors (Sigma). The cells were incubated on a heating block at 95 °C for 5 min and then sonicated for 20 min. The extracted proteins were quantified with a BCA Protein Assay Kit, reduced with 10 mM dithiothreitol (DTT) for 30 min, alkylated with 50 mM iodoacetamide (IAA) for 30 min in the dark, diluted 5-fold with 50 mM ammonium bicarbonate, and digested with Lys-C for 3 h at room temperature and with trypsin overnight at room temperature. After digestion, 1 mL of ethyl acetate was added and the mixture was acidified with 0.5% trifluoroacetic acid (TFA) (final concentration). The samples were agitated for 2 min and centrifuged at 15,800g for 2 min to completely separate the aqueous and organic phases. The aqueous phase was collected and desalted using StageTips[42] with SDB-XC Empore disk membranes.

Phosphopeptide Enrichment.

Metal oxide chromatographic (MOC) tips were prepared as described previously.[43] Briefly, C8 StageTips packed with titania beads (0.5 mg/50 μg of digests) were equilibrated with 80% acetonitrile (ACN) containing 0.1% TFA and 300 mg/mL lactic acid as a selectivity enhancer (solution A). The digested samples (50 μg/50 μL) were diluted with an equal amount of solution A and loaded onto the MOC tips. After washes with solution A and 80% ACN with 0.1% TFA, phosphopeptides were eluted with 0.5% piperidine. The eluate was acidified by adding 10% TFA to the final concentration of 0.1% and desalted using SDB-XC StageTips. For solid-phase TMT labeling, 10% TFA was replaced with 10% heptafluorobutyric acid (HFBA) and the mixture was loaded onto the StageTip-based micro-reactor.

Solution-Phase TMT Labeling.

Digested peptides or enriched phosphopeptides were dried and resuspended in 200 mM 4-(2-hydroxyethyl)-1-piperazineethanesulfonic acid (HEPES) pH 8.5, mixed with TMTzero or TMT10plex label reagent dissolved in acetonitrile, and left to incubate for 1 h at room temperature. The reactions were quenched by the addition of hydroxylamine to give a final concentration of 0.33%. Then the samples were acidified, diluted to make the acetonitrile

concentration less than 5%, and desalted using SDB-XC StageTips. Aliquots of 50 µg digest were labeled in a final volume of 55 µL, consisting of 50 µL of the sample in the buffer and 5 µL of 100 µg TMT reagent in ACN. Samples after phosphopeptide enrichment were labeled in a final volume of 10 µL consisting of 5 µL of the sample in the buffer and 5 µL of ACN with 25 µg TMT reagent.

Solid-Phase TMT Labeling.

SDB-XC StageTips packed with chromatographic sorbent (0.5 mg) were activated with 80% acetonitrile (ACN) with 0.1% TFA and equilibrated with 5% ACN with 0.1% TFA. Then the phosphopeptides were loaded onto each tip and washed with a 50 mM phosphate buffer (pH 6.5). TMT reagent was dissolved in ACN and diluted with 50 mM phosphate buffer to reduce the acetonitrile content to less than 5% in order to avoid peptide elution. 10 µL of this TMT solution (10 µg/10 µL) was loaded onto each tip. Samples were left on the reactor tip for 1 hour at RT. During incubation, the particles were kept wet. After 1 h, the reactor tip was washed with 5% ACN with 0.1% TFA and the peptides were eluted with 80% ACN with 0.1% TFA.

NanoLC/MS/MS Analyses.

NanoLC/MS/MS analyses of synthetic phosphopeptides were performed on an LTQ (Thermo Fisher Scientific, Bremen, Germany) connected to a Thermo Ultimate 3000 nanoflow pump and an HTC-PAL autosampler (CTC Analytics, Zwingen, Switzerland). For HeLa proteome analysis, a Q Exactive mass spectrometer (Thermo Scientific) equipped with an UltiMate 3000 RSLCnano pump and an HTC-PAL autosampler was employed. A 15 cm column with a 100 µm inner diameter in-house-packed with 3 µm reversed-phase silica beads (ReproSil-Pur C18-AQ, Dr. Maisch) was used for method evaluation. The mobile phases consisted of (A) 0.5% acetic acid and (B) 0.5% acetic acid and 80% acetonitrile. A 20 min or 65 min linear gradient ranging from 5% to 40% B was employed. The spray voltage was set to 2400 V and the heated capillary temperature was set to 240 °C. The injection volume was 5 µL, and the flow rate was 500 nL/min. The top 10 precursor ions were selected in each MS scan for subsequent MS/MS scans. Full scan resolution was set to 70,000 at m/z 200. The mass range was set to 300-1500. The resolution and AGC target for MS2 scans were set at 35,000 and 1e5, respectively. Isolation width was set at 1.4 Th. The normalized collision energy was set at 33. Only charge states 2-5 were targeted for MS2. All data were acquired in profile mode using positive polarity, and the lock mass function was used to obtain constant mass accuracy during the analysis.[44]

A MonoCap C18 High Resolution 2000 (100 µm i.d., 200 cm) (GL Sciences) was employed for single-shot in-depth phosphoproteome analysis, under essentially the same conditions as

described above, but with the following changes: 480 min linear gradient ranging from 5% to 40% B, spray voltage 3200 V, MS1 mass range 350-1500, normalized collision energy 32, and dynamic exclusion 40 sec.

Database Searching for Method Evaluation.

Peptides and proteins were identified by means of automated database searching using Mascot v2.5 (Matrix Science, London) against UniprotKB/Swissprot release 2015_01 or 2016_03 with a precursor mass tolerance of 5 ppm, a fragment ion mass tolerance of 0.02 Da, and strict Trypsin/P specificity allowing for up to 2 missed cleavages. Carbamidomethyl (C), TMT or TMT6plex (K), and TMT or TMT6plex (N-Term) were set as fixed modifications. Oxidation (M) and phosphorylation (STY) were allowed as variable modifications. For checking labeling efficiency, carbamidomethyl (C) was set as a fixed modification, and oxidation (M), phosphorylation (STY), TMT (K), and TMT (N-Term) were allowed as variable modifications. Peptides were considered identified if the Mascot score was over the 95% confidence limit ($p < 0.05$) for each peptide.

Database Searching for Differential Analysis of Selumetinib-treated HeLa Cells.

Peptides and proteins were identified by means of automated database searching using Mascot v2.7 against UniprotKB/Swissprot release 2019_10 with a precursor mass tolerance of 5 ppm, a fragment ion mass tolerance of 0.02 Da, and strict Trypsin/P specificity allowing for up to 2 missed cleavages. Carbamidomethyl (C), TMT6plex (K), and TMT6plex (N-Term) were set as fixed modifications. Oxidation (M) and phosphorylation (STY) were allowed as variable modifications. Percolator[45] on Proteome Discoverer (version 2.1) was used for validation of peptide spectrum matches (PSMs) and peptide groups with a 1% false discovery rate (FDR) based on q values. PhosphoRS (ptmRS)[46] was utilized to evaluate phosphorylation site localization confidence.

Data availability

The MS raw data and analysis files have been deposited with the ProteomeXchange Consortium (http://proteomecentral.proteomexchange.org) via the jPOST partner repository[47,48] (https:// jpostdb.org) with the data set identifier PXD025536.

■ RESULTS AND DISCUSSION

Combining TMT labeling with TiO_2-based phosphopeptide enrichment

In phosphoproteomics studies, quantitative tag labeling such as TMT is often performed prior to the enrichment of phosphopeptides to account for operational variability. However, the effect of chemical labeling on the enrichment process of phosphopeptides with TiO_2 chromatography has not been systematically studied; when a new labeling reagent such as TMTpro[49] is introduced, the enrichment process of phosphopeptides needs to be re-examined. On the other hand, chemical labeling after phosphopeptide enrichment eliminates the need for reexamination. In addition, the amount of peptide can be significantly reduced, and the cost of labeling reagents can be reduced accordingly. In order to determine whether phosphopeptide enrichment or TMT labeling should be done first when analyzing relatively small samples, the following experiment was performed. First, 50 μg of digested peptide was labeled with 100 μg of TMT in solution, and phosphopeptides were enriched from the TMT-labeled digest (TMT-TiO_2). Next, phosphopeptides were enriched from 50 μg of peptides and labeled with 25 μg of TMT in solution (TiO_2-TMT). Each sample enriched with phosphopeptides was labeled with a different TMT tag, mixed in equal amounts, and analyzed by nanoLC/MS/MS (Figure 1A).

Figure 1B shows the distribution of the reporter ion intensities of quantified phosphopeptides. The TiO_2-TMT strategy outperformed the TMT-TiO_2 strategy in terms of the recovery of phosphopeptides, despite the smaller-scale TMT labeling reaction in the TiO_2-TMT strategy, which often leads to loss of samples. The TiO_2-TMT strategy gave 5.4-fold higher signals for reporter ions on average. We examined the reasons for the low recovery in the TMT-TiO_2 workflow and found that the intensity ratios between the two approaches were correlated with the number of phosphorylation sites per peptide (Figure 1C left). The same tendency was observed for the number of acidic residues (Glu, Asp) per peptide (Figure 1C right), suggesting that TMT-labeled phosphopeptides need more acidic residues than unlabeled ones in order to be enriched by TiO_2 chromatography. To verify if TMT-labeled phosphopeptides have weaker affinity for TiO_2, we prepared phosphopeptide samples with and without TMT, collected both flow-through and elution fractions of TiO_2 chromatography, and analyzed them using nanoLC/MS/MS. As a result, approximately 10% of TMT-labeled phosphopeptides were in the flow-through fraction whereas less than 1% of unlabeled phosphopeptides were found in the flow-through fraction (Figure S1), indicating that the low recovery in the TMT-TiO_2 workflow was caused by the weaker affinity of TMT-labeled phosphopeptides for TiO_2 beads. This may be due to the undesirable charge enhancement effect of the TMT-tag[50], in which the tertiary amino group of TMT may form an intramolecular salt bridge with phosphate and inhibit the interaction between phosphate and TiO_2 beads. We also compared the reproducibility of these two strategies in triplicate analyses. To our surprise,

the reproducibility of the TiO_2-TMT strategy was superior to that of the TMT-TiO_2 strategy. More than 90% of quantified phosphopeptides in the TiO_2-TMT strategy have a relative standard deviation value of less than 20%, indicating that technical variation in the phosphopeptide enrichment procedure doesn't significantly affect the quantitation (Figure 1D). The lower reproducibility of the TMT-TiO_2 strategy might be due to the lower signal intensity of reporter ions. From these results, we conclude that TMT labeling should be performed after phosphopeptide enrichment to minimize sample loss, especially for small amounts of samples.

Development of solid-phase TMT labeling protocol for small amounts of phosphopeptides

Since the elution buffer for TiO_2 chromatography is not compatible with the TMT labeling buffer, a buffer exchange step is required before the labeling reaction. To avoid potential loss of phosphopeptides, we examined the use of a single StageTip-based reversed-phase column as a desalting device as well as a solid phase reactor for nanogram-scale amounts of phosphopeptides.

First, we optimized the pH condition for the StageTip-based reaction. 20 pmol (less than 25 ng) of a model synthetic phosphopeptide (YLpSFTPPEK) was labeled with 10 μg of TMTzero reagent using a StageTip packed with C18 membrane as a reactor. At pH 4.5, about 30% of the peptide was unlabeled, and 60% had only one of the two amino groups labeled with TMT, whereas at pH 6.5, more than 95% of the peptide was completely labeled (Fig. 2A). Fig. 2B shows the chromatogram of the reaction samples at pH 4.5 and 6.5. A doublet peak corresponding to the partially labeled peptide was observed in the extracted ion chromatogram (XIC) at pH 4.5, indicating the presence of both N-terminal and lysine-labeled peptides. On the other hand, at pH 6.5, a single peak corresponding to the completely labeled peptide was predominantly observed even when the same amount of TMT reagent was used. Although several groups have employed pH 4.5 for solid-phase TMT labeling for larger-scale reactions such as 1 μg of peptides with 40 μg TMT,[37,38] we found that pH 4.5 was too low to label a nanogram-scale amount of peptides with TMT reagents. Based on these results, we chose pH 6.5 for further investigation, using as little TMT reagent as possible.

Second, we investigated chromatographic sorbents for solid-phase labeling. Reversed-phase C18-silica gel (Sep-Pak tC18) as well as a variety of polymer-based sorbents were evaluated. Phosphopeptides enriched from 50 μg of HeLa digests were labeled with 10 μg of TMTzero. Among the five materials examined, C18-silica and C18-modified poly(styrene-divinylbenzene) co-polymer particles (C18-polymer, InertSep RP-C18) gave higher labeling efficiency, while other polymer particles without the C18 moiety were not effective (Figure 3A). To examine the reason for the lower labeling efficiency, we further focused on unlabeled phosphopeptides and found that these phosphopeptides are more hydrophilic, based on the

peptide grand average of hydropathicity index (GRAVY index[51]) (Figure 3B), suggesting that these hydrophilic phosphopeptides were not completely trapped at the inlet of the StageTip column when the sorbents were insufficiently hydrophobic to concentrate them within a narrow sample band. Therefore, the C18-polymer sorbent, which is expected to have the most hydrophobic character, gave the best results in terms of the labeling efficiency among these 5 sorbents. Notably, C18-polymer also gave the best results in terms of the number of identified phosphopeptides (Figure 3C). Thus, we chose the StageTip packed with this C18-polymer sorbent for further analysis (Figure S2).

We also compared our StageTip-based protocol with the conventional in-solution protocol using phosphopeptides with a wide range of hydrophobicity to examine whether any bias is introduced. As a result, our StageTip-based protocol gave 1.26 times better results than the in-solution protocol on average (Figure 4A), while the first-eluted fraction gave worse results in the StageTip protocol than in the in-solution protocol, as shown in Figure 4B. It has already been reported that lower recovery of hydrophilic peptides was observed when a solid-phase cartridge was used.[37,52] To improve the recovery of these hydrophilic phosphopeptides, the use of more hydrophobic ion-pairing reagents than TFA as loading buffer additives for StageTip was investigated.[53,54] We selected HFBA based on its strong hydrophobicity and compatibility with LC/MS, and compared it with the original TFA-StageTip protocol as well as the in-solution protocol. As a result, this HFBA-StageTip protocol gave 1.71 times higher signals than the in-solution protocol on average (Figure 4A). Even for the first-eluted fraction, the HFBA protocol gave comparable results with the in-solution protocol (Figure 4C). Moreover, HFBA also increased the recovery of hydrophobic phosphopeptides (Figure 4D), possibly by preventing adsorption of phosphopeptides on the plastic labware, because HFBA has a stronger surface activity than TFA.[55] We further confirmed the linearity range of the optimized method using phosphopeptides enriched from 1 - 100 µg of HeLa proteins (Figure S3). Considering that the content of phosphopeptides is approximately 0.5% of the total tryptic peptides from HeLa cells (estimated by nanoLC/UV214nm, data not shown), this method can be used for the analysis of 5 – 500 ng of phosphopeptides. We concluded that the use of StageTip with C18-polymer sorbent together with HFBA as the loading buffer additive, operated at pH 6.5, is the optimum condition for StageTip-based nano-scale solid-phase labeling of phosphopeptides. We also confirmed that this protocol is compatible with newly commercialized TMTpro reagents (Figure S4).

Phosphoproteome Analysis of Selumetinib-treated HeLa cells.

To demonstrate the utility of the established nano-scale TMT labeling strategy, we applied it to phosphoproteome profiling of selumetinib-treated HeLa cells. In triplicate nanoLC/MS/MS runs utilizing a two-meter-long monolithic silica capillary column with an 8-hour gradient, we

successfully quantified 9,822 phosphopeptides enriched from 50 μg of HeLa cell whole digests per TMT channel (Figure 5A). The required TMT reagent amount was 10 μg per channel and 10-plexed TMT reagents were used (selumetinib-treated, n = 5 and DMSO-treated, n = 5). The quantified phosphopeptides are summarized in Supplemental Table S1. From these phosphopeptides, peptides with phosphosite localization probability > 75% (n = 7,524) were used for further analysis, resulting in the identification of 7428 Class I phosphosites[56]. Using Perseus software, we identified 305 phosphopeptides that were significantly downregulated by selumetinib treatment[57] (Figure 5B). Approximately 4% of all phosphopeptides showed a significant decrease (Figure 5B and Table S1).

Selumetinib is known to inhibit the activity of MAP kinase kinase 1 and 2 (MKK1/2), and thus inhibits the activity of their downstream extracellular signal-related kinases 1 and 2 (ERK1/2)[58]. A previous phosphoproteomics study on melanoma cells found that MKK1/2 inhibitor treatment resulted in almost the same phosphoproteome changes as ERK1/2 inhibitor treatment[59]. This indicates that there are almost no branched pathways at the level of MKK1/2. In our study, phosphopeptides corresponding to the regulatory site of ERK1/2, and the known downstream substrates of ERK1/2 such as MYC, STMN1, and RPS6KA1 showed a significant decrease upon selumetinib treatment. In addition, nucleoporin complex members, which were previously shown to be phosphorylated in an ERK-dependent manner,[60,61] also showed a decrease upon selumetinib treatment (Figure S5).

Next, we performed Kinase Set Enrichment Analysis (KSEA)[62]. Kinase–substrate links were assigned based on the kinase substrate dataset from PhosphoSitePlus. As expected, KSEA showed downregulation of MKK1, ERK2, and RPS6KA1. Interestingly, some kinases, such as MTOR and CDK4, were activated after selumetinib treatment. It has been reported that the PI3K/MTOR pathway is activated after MAPK pathway inhibition in some cell lines,[63,64] and the co-inhibition of MAPK and MTOR showed synergistic effects[65]. MEK/CDK4,6 co-inhibition is also effective in some melanomas[66]. Collectively, our results successfully re-capture the major kinase activity changes caused by the drug treatment. Thus, overall, this strategy enables phosphoproteomic profiling of the kinase inhibitor with minimal amounts of phosphopeptides and TMT reagents.

■ CONCLUSIONS

We developed a new strategy for highly sensitive phosphoproteome analysis using nano-scale solid-phase TMT labeling after phosphopeptide enrichment. The appropriate choice of reaction pH, reversed-phase sorbent, and ion-pairing reagent is the key to the successful labeling of phosphopeptides on the solid-phase micro-reactor. Our method requires only a tiny amount of TMT reagents for labeling phosphopeptides without loss of sensitivity, owing to the use of highly sensitive StageTip-based isobaric labeling technology after phosphopeptide

enrichment. We envision that the present strategy will be useful for large-scale phosphoproteomics studies with nanogram-scale TMT labeling.

■ ASSOCIATED CONTENT

Supporting Information.

The Supporting Information is available free of charge on the ACS Publications website http://pubs.acs.org

Figure S1, Recovery of TMT-labeled phosphopeptides in TiO2-based phosphopeptide enrichment; Figure S2, Photograph of a StageTip used for solid-phase TMT labeling; Figure S3, Evaluation of quantitative linearity of the optimized solid-phase TMT labeling method; Figure S4, Labeling efficiency of solid-phase TMTpro labeling; Figure S5, STRING network analysis of proteins having decreased phosphopeptides upon selumetinib treatment. (PDF)

Table S1, Identified phosphopeptides and TMT intensities (XLSX)

■ AUTHOR INFORMATION

Corresponding Author

Yasushi Ishihama − Department of Molecular and Cellular BioAnalysis, Graduate School of Pharmaceutical Sciences, Kyoto University, Kyoto 606-8501, Japan; Laboratory of Clinical and Analytical Chemistry, National Institute of Biomedical Innovation, Health and Nutrition, Ibaraki, Osaka, 567-0085, Japan; orcid.org/0000-0001-7714-203X; Email: yishiham@pharm.kyoto-u.ac.jp

Author

Kosuke Ogata − Department of Molecular and Cellular BioAnalysis, Graduate School of Pharmaceutical Sciences, Kyoto University, Kyoto 606-8501, Japan; orcid.org/0000-0002-0634-3990

Chia-Feng Tsai − Department of Molecular and Cellular BioAnalysis, Graduate School of Pharmaceutical Sciences, Kyoto University, Kyoto 606-8501, Japan; orcid.org/0000-0002-6514-6911

Present Address

Chia-Feng Tsai − Biological Sciences Division, Pacific Northwest National Laboratory, Richland, Washington 99354, USA

Notes

The authors declare no competing financial interest.

■ ACKNOWLEDGMENTS

We would like to thank members of Department of Molecular & Cellular BioAnalysis for fruitful discussion. This work was supported by JST Strategic Basic Research Program CREST (No. 18070870), JSPS Grant-in-Aid for JSPS Fellows No. 15F15343, JSPS Grants-in-Aid for Scientific Research No. 17H03605 and 21H02459, and JSPS Grant-in-Aid for Challenging Research (Exploratory) No. 20K21478.

References

(1) Hunter, T. Tyrosine Phosphorylation: Thirty Years and Counting. *Curr. Opin. Cell Biol.* **2009**, *21* (2), 140–146.

(2) Pawson, T.; Scott, J. D. Signaling through Scaffold, Anchoring, and Adaptor Proteins. *Science* **1997**, *278* (5346), 2075–2080.

(3) Hebert, A. S.; Richards, A. L.; Bailey, D. J.; Ulbrich, A.; Coughlin, E. E.; Westphall, M. S.; Coon, J. J. The One Hour Yeast Proteome. *Mol. Cell. Proteomics* **2014**, *13* (1), 339–347.

(4) Bekker-Jensen, D. B.; Martínez-Val, A.; Steigerwald, S.; Rüther, P.; Fort, K. L.; Arrey, T. N.; Harder, A.; Makarov, A.; Olsen, J. V. A Compact Quadrupole-Orbitrap Mass Spectrometer with FAIMS Interface Improves Proteome Coverage in Short LC Gradients. *Mol. Cell. Proteomics* **2020**, *19* (4), 716–729.

(5) Meier, F.; Brunner, A.-D.; Koch, S.; Koch, H.; Lubeck, M.; Krause, M.; Goedecke, N.; Decker, J.; Kosinski, T.; Park, M. A.; Bache, N.; Hoerning, O.; Cox, J.; Räther, O.; Mann, M. Online Parallel Accumulation-Serial Fragmentation (PASEF) with a Novel Trapped Ion Mobility Mass Spectrometer. *Mol. Cell. Proteomics* **2018**, *17* (12), 2534–2545.

(6) Scheltema, R. A.; Hauschild, J.-P.; Lange, O.; Hornburg, D.; Denisov, E.; Damoc, E.; Kuehn, A.; Makarov, A.; Mann, M. The Q Exactive HF, a Benchtop Mass Spectrometer with a Pre-Filter, High-Performance Quadrupole and an Ultra-High-Field Orbitrap Analyzer. *Mol. Cell. Proteomics* **2014**, *13* (12), 3698–3708.

(7) MacNair, J. E.; Patel, K. D.; Jorgenson, J. W. Ultrahigh-Pressure Reversed-Phase Capillary Liquid Chromatography: Isocratic and Gradient Elution Using Columns Packed with 1.0-Micron Particles. *Anal. Chem.* **1999**, *71* (3), 700–708.

(8) Mellors, J. S.; Jorgenson, J. W. Use of 1.5-Microm Porous Ethyl-Bridged Hybrid Particles as a Stationary-Phase Support for Reversed-Phase Ultrahigh-Pressure Liquid Chromatography. *Anal. Chem.* **2004**, *76* (18), 5441–5450.

(9) Patel, K. D.; Jerkovich, A. D.; Link, J. C.; Jorgenson, J. W. In-Depth Characterization of Slurry Packed Capillary Columns with 1.0-Microm Nonporous Particles Using Reversed-Phase Isocratic Ultrahigh-Pressure Liquid Chromatography. *Anal. Chem.* **2004**, *76* (19), 5777–5786.

(10) Iwasaki, M.; Sugiyama, N.; Tanaka, N.; Ishihama, Y. Human Proteome Analysis by Using Reversed Phase Monolithic Silica Capillary Columns with Enhanced Sensitivity. *J. Chromatogr. A* **2012**, *1228*, 292–297.

(11) Luo, Q.; Shen, Y.; Hixson, K. K.; Zhao, R.; Yang, F.; Moore, R. J.; Mottaz, H. M.; Smith, R. D. Preparation of 20-Microm-I.d. Silica-Based Monolithic Columns and Their Performance for Proteomics Analyses. *Anal. Chem.* **2005**, *77* (15), 5028–5035.

(12) Kobayashi, H.; Ikegami, T.; Kimura, H.; Hara, T.; Tokuda, D.; Tanaka, N. Properties of Monolithic Silica Columns for HPLC. *Anal. Sci.* **2006**, *22* (4), 491–501.

(13) He, B.; Tait, N.; Regnier, F. Fabrication of Nanocolumns for Liquid Chromatography. *Anal. Chem.* **1998**, *70* (18), 3790–3797.

(14) Baca, M.; Desmet, G.; Ottevaere, H.; De Malsche, W. Achieving a Peak Capacity of 1800 Using an 8 M Long Pillar Array Column. *Anal. Chem.* **2019**, *91* (17), 10932–10936.

(15) Ficarro, S. B.; McCleland, M. L.; Stukenberg, P. T.; Burke, D. J.; Ross, M. M.; Shabanowitz, J.; Hunt, D. F.; White, F. M. Phosphoproteome Analysis by Mass Spectrometry and Its Application to Saccharomyces Cerevisiae. *Nat. Biotechnol.* **2002**, *20* (3), 301–305.

(16) Stensballe, A.; Andersen, S.; Jensen, O. N. Characterization of Phosphoproteins from Electrophoretic Gels by Nanoscale Fe(III) Affinity Chromatography with off-Line Mass Spectrometry Analysis. *Proteomics* **2001**, *1* (2), 207–222.

(17) Ikeguchi, Y.; Nakamura, H. Determination of Organic Phosphates by Column-Switching High Performance Anion-Exchange Chromatography Using On-Line Preconcentration on Titania. *Anal. Sci.* **1997**, *13* (3), 479–483.

(18) Kweon, H. K.; Håkansson, K. Selective Zirconium Dioxide-Based Enrichment of Phosphorylated Peptides for Mass Spectrometric Analysis. *Anal. Chem.* **2006**, *78* (6), 1743–1749.
(19) Wolschin, F.; Wienkoop, S.; Weckwerth, W. Enrichment of Phosphorylated Proteins and Peptides from Complex Mixtures Using Metal Oxide/hydroxide Affinity Chromatography (MOAC). *Proteomics* **2005**, *5* (17), 4389–4397.
(20) Rauniyar, N.; Yates, J. R., 3rd. Isobaric Labeling-Based Relative Quantification in Shotgun Proteomics. *J. Proteome Res.* **2014**, *13* (12), 5293–5309.
(21) Ting, L.; Rad, R.; Gygi, S. P.; Haas, W. MS3 Eliminates Ratio Distortion in Isobaric Multiplexed Quantitative Proteomics. *Nat. Methods* **2011**, *8* (11), 937–940.
(22) McAlister, G. C.; Nusinow, D. P.; Jedrychowski, M. P.; Wühr, M.; Huttlin, E. L.; Erickson, B. K.; Rad, R.; Haas, W.; Gygi, S. P. MultiNotch MS3 Enables Accurate, Sensitive, and Multiplexed Detection of Differential Expression across Cancer Cell Line Proteomes. *Anal. Chem.* **2014**, *86* (14), 7150–7158.
(23) Schweppe, D. K.; Eng, J. K.; Yu, Q.; Bailey, D.; Rad, R.; Navarrete-Perea, J.; Huttlin, E. L.; Erickson, B. K.; Paulo, J. A.; Gygi, S. P. Full-Featured, Real-Time Database Searching Platform Enables Fast and Accurate Multiplexed Quantitative Proteomics. *J. Proteome Res.* **2020**, *19* (5), 2026–2034.
(24) Schweppe, D. K.; Prasad, S.; Belford, M. W.; Navarrete-Perea, J.; Bailey, D. J.; Huguet, R.; Jedrychowski, M. P.; Rad, R.; McAlister, G.; Abbatiello, S. E.; Woulters, E. R.; Zabrouskov, V.; Dunyach, J.-J.; Paulo, J. A.; Gygi, S. P. Characterization and Optimization of Multiplexed Quantitative Analyses Using High-Field Asymmetric-Waveform Ion Mobility Mass Spectrometry. *Anal. Chem.* **2019**, *91* (6), 4010–4016.
(25) Pfammatter, S.; Bonneil, E.; Thibault, P. Improvement of Quantitative Measurements in Multiplex Proteomics Using High-Field Asymmetric Waveform Spectrometry. *J. Proteome Res.* **2016**, *15* (12), 4653–4665.
(26) Ogata, K.; Ishihama, Y. Extending the Separation Space with Trapped Ion Mobility Spectrometry Improves the Accuracy of Isobaric Tag-Based Quantitation in Proteomic LC/MS/MS. *Anal. Chem.* **2020**, *92* (12), 8037–8040.
(27) Yi, L.; Tsai, C.-F.; Dirice, E.; Swensen, A. C.; Chen, J.; Shi, T.; Gritsenko, M. A.; Chu, R. K.; Piehowski, P. D.; Smith, R. D.; Rodland, K. D.; Atkinson, M. A.; Mathews, C. E.; Kulkarni, R. N.; Liu, T.; Qian, W.-J. Boosting to Amplify Signal with Isobaric Labeling (BASIL) Strategy for Comprehensive Quantitative Phosphoproteomic Characterization of Small Populations of Cells. *Anal. Chem.* **2019**, *91* (9), 5794–5801.
(28) Budnik, B.; Levy, E.; Harmange, G.; Slavov, N. SCoPE-MS: Mass Spectrometry of Single Mammalian Cells Quantifies Proteome Heterogeneity during Cell Differentiation. *Genome Biol.* **2018**, *19* (1), 161.
(29) Cheung, T. K.; Lee, C.-Y.; Bayer, F. P.; McCoy, A.; Kuster, B.; Rose, C. M. Defining the Carrier Proteome Limit for Single-Cell Proteomics. *Nat. Methods* **2021**, *18* (1), 76–83.
(30) Huang, F.-K.; Zhang, G.; Lawlor, K.; Nazarian, A.; Philip, J.; Tempst, P.; Dephoure, N.; Neubert, T. A. Deep Coverage of Global Protein Expression and Phosphorylation in Breast Tumor Cell Lines Using TMT 10-Plex Isobaric Labeling. *J. Proteome Res.* **2017**, *16* (3), 1121–1132.
(31) Navarrete-Perea, J.; Yu, Q.; Gygi, S. P.; Paulo, J. A. Streamlined Tandem Mass Tag (SL-TMT) Protocol: An Efficient Strategy for Quantitative (Phospho)proteome Profiling Using Tandem Mass Tag-Synchronous Precursor Selection-MS3. *J. Proteome Res.* **2018**, *17* (6), 2226–2236.
(32) Lombardi, B.; Rendell, N.; Edwards, M.; Katan, M.; Zimmermann, J. G. Evaluation of Phosphopeptide Enrichment Strategies for Quantitative TMT Analysis of Complex Network Dynamics in Cancer-Associated Cell Signalling. *EuPA Open Proteom* **2015**, *6*, 10–15.
(33) Paulo, J. A.; Navarrete-Perea, J.; Erickson, A. R.; Knott, J.; Gygi, S. P. An Internal Standard for Assessing Phosphopeptide Recovery from Metal Ion/Oxide Enrichment Strategies. *J. Am. Soc. Mass Spectrom.* **2018**, *29* (7), 1505–1511.

(34) Zecha, J.; Satpathy, S.; Kanashova, T.; Avanessian, S. C.; Kane, M. H.; Clauser, K. R.; Mertins, P.; Carr, S. A.; Kuster, B. TMT Labeling for the Masses: A Robust and Cost-Efficient, In-Solution Labeling Approach. *Mol. Cell. Proteomics* **2019**, *18* (7), 1468–1478.
(35) Erickson, B. K.; Jedrychowski, M. P.; McAlister, G. C.; Everley, R. A.; Kunz, R.; Gygi, S. P. Evaluating Multiplexed Quantitative Phosphopeptide Analysis on a Hybrid Quadrupole Mass Filter/linear Ion Trap/orbitrap Mass Spectrometer. *Anal. Chem.* **2015**, *87* (2), 1241–1249.
(36) Hogrebe, A.; von Stechow, L.; Bekker-Jensen, D. B.; Weinert, B. T.; Kelstrup, C. D.; Olsen, J. V. Benchmarking Common Quantification Strategies for Large-Scale Phosphoproteomics. *Nat. Commun.* **2018**, *9* (1), 1045.
(37) Böhm, G.; Prefot, P.; Jung, S.; Selzer, S.; Mitra, V.; Britton, D.; Kuhn, K.; Pike, I.; Thompson, A. H. Low-pH Solid-Phase Amino Labeling of Complex Peptide Digests with TMTs Improves Peptide Identification Rates for Multiplexed Global Phosphopeptide Analysis. *J. Proteome Res.* **2015**, *14* (6), 2500–2510.
(38) de Graaf, E. L.; Pellegrini, D.; McDonnell, L. A. Set of Novel Automated Quantitative Microproteomics Protocols for Small Sample Amounts and Its Application to Kidney Tissue Substructures. *J. Proteome Res.* **2016**, *15* (12), 4722–4730.
(39) Myers, S. A.; Rhoads, A.; Cocco, A. R.; Peckner, R.; Haber, A. L.; Schweitzer, L. D.; Krug, K.; Mani, D. R.; Clauser, K. R.; Rozenblatt-Rosen, O.; Hacohen, N.; Regev, A.; Carr, S. A. Streamlined Protocol for Deep Proteomic Profiling of FAC-Sorted Cells and Its Application to Freshly Isolated Murine Immune Cells. *Mol. Cell. Proteomics* **2019**, *18* (5), 995–1009.
(40) Mao, Y.; Chen, P.; Ke, M.; Chen, X.; Ji, S.; Chen, W.; Tian, R. Fully Integrated and Multiplexed Sample Preparation Technology for Sensitive Interactome Profiling. *Anal. Chem.* **2021**, *93* (5), 3026–3034.
(41) Masuda, T.; Tomita, M.; Ishihama, Y. Phase Transfer Surfactant-Aided Trypsin Digestion for Membrane Proteome Analysis. *J. Proteome Res.* **2008**, *7* (2), 731–740.
(42) Rappsilber, J.; Mann, M.; Ishihama, Y. Protocol for Micro-Purification, Enrichment, Pre-Fractionation and Storage of Peptides for Proteomics Using StageTips. *Nat. Protoc.* **2007**, *2* (8), 1896–1906.
(43) Sugiyama, N.; Masuda, T.; Shinoda, K.; Nakamura, A.; Tomita, M.; Ishihama, Y. Phosphopeptide Enrichment by Aliphatic Hydroxy Acid-Modified Metal Oxide Chromatography for Nano-LC-MS/MS in Proteomics Applications. *Mol. Cell. Proteomics* **2007**, *6* (6), 1103–1109.
(44) Olsen, J. V.; de Godoy, L. M. F.; Li, G.; Macek, B.; Mortensen, P.; Pesch, R.; Makarov, A.; Lange, O.; Horning, S.; Mann, M. Parts per Million Mass Accuracy on an Orbitrap Mass Spectrometer via Lock Mass Injection into a C-Trap. *Mol. Cell. Proteomics* **2005**, *4* (12), 2010–2021.
(45) Käll, L.; Canterbury, J. D.; Weston, J.; Noble, W. S.; MacCoss, M. J. Semi-Supervised Learning for Peptide Identification from Shotgun Proteomics Datasets. *Nat. Methods* **2007**, *4* (11), 923–925.
(46) Taus, T.; Köcher, T.; Pichler, P.; Paschke, C.; Schmidt, A.; Henrich, C.; Mechtler, K. Universal and Confident Phosphorylation Site Localization Using phosphoRS. *J. Proteome Res.* **2011**, *10* (12), 5354–5362.
(47) Okuda, S.; Watanabe, Y.; Moriya, Y.; Kawano, S.; Yamamoto, T.; Matsumoto, M.; Takami, T.; Kobayashi, D.; Araki, N.; Yoshizawa, A. C.; Tabata, T.; Sugiyama, N.; Goto, S.; Ishihama, Y. jPOSTrepo: An International Standard Data Repository for Proteomes. *Nucleic Acids Res.* **2017**, *45* (D1), D1107–D1111.
(48) Moriya, Y.; Kawano, S.; Okuda, S.; Watanabe, Y.; Matsumoto, M.; Takami, T.; Kobayashi, D.; Yamanouchi, Y.; Araki, N.; Yoshizawa, A. C.; Tabata, T.; Iwasaki, M.; Sugiyama, N.; Tanaka, S.; Goto, S.; Ishihama, Y. The jPOST Environment: An Integrated Proteomics Data Repository and Database. *Nucleic Acids Res.* **2019**, *47* (D1), D1218–D1224.
(49) Thompson, A.; Wölmer, N.; Koncarevic, S.; Selzer, S.; Böhm, G.; Legner, H.; Schmid, P.; Kienle, S.; Penning, P.; Höhle, C.; Berfelde, A.; Martinez-Pinna, R.;

Farztdinov, V.; Jung, S.; Kuhn, K.; Pike, I. TMTpro: Design, Synthesis, and Initial Evaluation of a Proline-Based Isobaric 16-Plex Tandem Mass Tag Reagent Set. *Anal. Chem.* **2019**, *91* (24), 15941–15950.

(50) Thingholm, T. E.; Palmisano, G.; Kjeldsen, F.; Larsen, M. R. Undesirable Charge-Enhancement of Isobaric Tagged Phosphopeptides Leads to Reduced Identification Efficiency. *J. Proteome Res.* **2010**, *9* (8), 4045–4052.

(51) Kyte, J.; Doolittle, R. F. A Simple Method for Displaying the Hydropathic Character of a Protein. *J. Mol. Biol.* **1982**, *157* (1), 105–132.

(52) Tsai, C.-F.; Smith, J. S.; Krajewski, K.; Zhao, R.; Moghieb, A. M.; Nicora, C. D.; Xiong, X.; Moore, R. J.; Liu, T.; Smith, R. D.; Jacobs, J. M.; Rajagopal, S.; Shi, T. Tandem Mass Tag Labeling Facilitates Reversed-Phase Liquid Chromatography-Mass Spectrometry Analysis of Hydrophilic Phosphopeptides. *Anal. Chem.* **2019**, *91* (18), 11606–11613.

(53) Dass, C.; Mahalakshmi, P.; Grandberry, D. Manipulation of Ion-Pairing Reagents for Reversed-Phase High-Performance Liquid Chromatographic Separation of Phosphorylated Opioid Peptides from Their Non-Phosphorylated Analogues. *J. Chromatogr. A* **1994**, *678* (2), 249–257.

(54) Ogata, K.; Krokhin, O. V.; Ishihama, Y. Retention Order Reversal of Phosphorylated and Unphosphorylated Peptides in Reversed-Phase LC/MS. *Anal. Sci.* **2018**, *34* (9), 1037–1041.

(55) Bhhatarai, B.; Gramatica, P. Prediction of Aqueous Solubility, Vapor Pressure and Critical Micelle Concentration for Aquatic Partitioning of Perfluorinated Chemicals. *Environ. Sci. Technol.* **2011**, *45* (19), 8120–8128.

(56) Olsen, J. V.; Blagoev, B.; Gnad, F.; Macek, B.; Kumar, C.; Mortensen, P.; Mann, M. Global, in Vivo, and Site-Specific Phosphorylation Dynamics in Signaling Networks. *Cell* **2006**, *127* (3), 635–648.

(57) Tyanova, S.; Temu, T.; Sinitcyn, P.; Carlson, A.; Hein, M. Y.; Geiger, T.; Mann, M.; Cox, J. The Perseus Computational Platform for Comprehensive Analysis of (prote)omics Data. *Nat. Methods* **2016**, *13* (9), 731–740.

(58) Davies, B. R.; Logie, A.; McKay, J. S.; Martin, P.; Steele, S.; Jenkins, R.; Cockerill, M.; Cartlidge, S.; Smith, P. D. AZD6244 (ARRY-142886), a Potent Inhibitor of Mitogen-Activated Protein Kinase/extracellular Signal-Regulated Kinase Kinase 1/2 Kinases: Mechanism of Action in Vivo, Pharmacokinetic/pharmacodynamic Relationship, and Potential for Combination in Preclinical Models. *Mol. Cancer Ther.* **2007**, *6* (8), 2209–2219.

(59) Basken, J.; Stuart, S. A.; Kavran, A. J.; Lee, T.; Ebmeier, C. C.; Old, W. M.; Ahn, N. G. Specificity of Phosphorylation Responses to Mitogen Activated Protein (MAP) Kinase Pathway Inhibitors in Melanoma Cells. *Mol. Cell. Proteomics* **2018**, *17* (4), 550–564.

(60) Kosako, H.; Yamaguchi, N.; Aranami, C.; Ushiyama, M.; Kose, S.; Imamoto, N.; Taniguchi, H.; Nishida, E.; Hattori, S. Phosphoproteomics Reveals New ERK MAP Kinase Targets and Links ERK to Nucleoporin-Mediated Nuclear Transport. *Nat. Struct. Mol. Biol.* **2009**, *16* (10), 1026–1035.

(61) Stuart, S. A.; Houel, S.; Lee, T.; Wang, N.; Old, W. M.; Ahn, N. G. A Phosphoproteomic Comparison of B-RAFV600E and MKK1/2 Inhibitors in Melanoma Cells. *Mol. Cell. Proteomics* **2015**, *14* (6), 1599–1615.

(62) Wiredja, D. D.; Koyutürk, M.; Chance, M. R. The KSEA App: A Web-Based Tool for Kinase Activity Inference from Quantitative Phosphoproteomics. *Bioinformatics* **2017**, *33* (21), 3489–3491.

(63) Hoeflich, K. P.; O'Brien, C.; Boyd, Z.; Cavet, G.; Guerrero, S.; Jung, K.; Januario, T.; Savage, H.; Punnoose, E.; Truong, T.; Zhou, W.; Berry, L.; Murray, L.; Amler, L.; Belvin, M.; Friedman, L. S.; Lackner, M. R. In Vivo Antitumor Activity of MEK and Phosphatidylinositol 3-Kinase Inhibitors in Basal-like Breast Cancer Models. *Clin. Cancer Res.* **2009**, *15* (14), 4649–4664.

(64) Sunayama, J.; Matsuda, K.-I.; Sato, A.; Tachibana, K.; Suzuki, K.; Narita, Y.; Shibui, S.; Sakurada, K.; Kayama, T.; Tomiyama, A.; Kitanaka, C. Crosstalk between the

PI3K/mTOR and MEK/ERK Pathways Involved in the Maintenance of Self-Renewal and Tumorigenicity of Glioblastoma Stem-like Cells. *Stem Cells* **2010**, *28* (11), 1930–1939.

(65) Holt, S. V.; Logie, A.; Davies, B. R.; Alferez, D.; Runswick, S.; Fenton, S.; Chresta, C. M.; Gu, Y.; Zhang, J.; Wu, Y.-L.; Wilkinson, R. W.; Guichard, S. M.; Smith, P. D. Enhanced Apoptosis and Tumor Growth Suppression Elicited by Combination of MEK (selumetinib) and mTOR Kinase Inhibitors (AZD8055). *Cancer Res.* **2012**, *72* (7), 1804–1813.

(66) Posch, C.; Sanlorenzo, M.; Ma, J.; Kim, S. T.; Zekhtser, M.; Ortiz-Urda, S. MEK/CDK4,6 Co-Targeting Is Effective in a Subset of NRAS, BRAF and “Wild Type” Melanomas. *Oncotarget* **2018**, *9* (79), 34990–34995.

Figure 1. Combining TMT labeling with TiO_2-based phosphopeptide enrichment workflow.

(A) Schematic representation of the workflow. TMT-labeled phosphopeptides from both methods were mixed in equal amounts and analyzed by LC/MS/MS. (B) Distribution of reporter ion intensities of identified phosphopeptides. TMT quantitation was performed only when the signals were detected in all 6 TMT channels. The box itself spans the interquartile range. The whiskers represent 5% and 95% quantiles. The thick horizontal line in each box indicates the median. (C) Relationship between reporter ion intensity ratios and the number of phosphorylations or acidic residues (Glu, Asp) on each phosphopeptide. The mono-phosphorylated peptides were harder to capture in the TMT-TiO_2 workflow. The box itself spans the interquartile range. The whiskers represent 5% and 95% quantiles. The thick horizontal line in each box indicates the median. (D) Frequency distribution of relative standard deviation (RSD) of identified phosphopeptide reporter ion intensities.

Figure 2. pH optimization of StageTip-based solid-phase TMT reaction.

(A) Peak area ratio of a synthetic phosphopeptide, YLpSFTPPEK. The peptide was categorized into three classes according to the number of TMT-tags. Not labeled: The peptide with no TMT-tag. Partially labeled: The peptide with a TMT-tag, but either the lysine side chain or peptide N-terminus is not labeled. Fully labeled: The peptide completely labeled with TMT. (B) Extracted ion chromatogram of synthetic phosphopeptide in each category.

Figure 3. Sorbent optimization for StageTip-based solid-phase TMT labeling.

(A) Screening of reversed-phase particles for solid-phase labeling. Each sorbent was evaluated in duplicate experiments. The sum of the phosphopeptide peak area is shown. Not labeled: The peptide with no TMT-tag. Partially labeled: The peptide with a TMT-tag but either the lysine side chain or peptide N-terminus is not labeled. Fully labeled: The peptide completely labeled with TMT. (B) GRAVY index distribution of identified phosphopeptides labeled with or without TMT from 5 different sorbents. (C) Phosphopeptide ID numbers from solid-phase labeling using different sorbents. Error bars show the standard deviation (n = 3).

Figure 4. Ion-pairing reagent optimization for StageTip-based solid-phase TMT labeling.

(A) Comparison of distributions of reporter ion intensity ratios between solution-phase and solid-phase labeling method with each ion-pairing reagent (n = 5, average). The box itself spans the interquartile range. The whiskers represent 5% and 95% quantiles. The thick horizontal line in each box indicates the median. (B-D) Relationship between reporter ion intensity ratio of phosphopeptides and their elution ACN composition in gradient analysis. (B)

Comparison between solid-phase TMT labeling with TFA and solution-phase labeling. (C) Comparison between solid-phase TMT labeling with HFBA and solution-phase labeling. (D) Comparison between solid-phase TMT labeling with HFBA and solid-phase TMT labeling with TFA. The box itself spans the interquartile range. The whiskers represent 5% and 95% quantiles. The thick horizontal line in each box indicates the median.

Figure 5. Differential analysis of selumetinib-treated HeLa phosphoproteomes.
(A) Schematic representation of the workflow. Control and selumetinib-treated HeLa cells were stimulated with EGF (15 min) and collected. After protein digestion, phosphopeptide enrichment and solid-phase TMT labeling, samples were analyzed in triplicate LC/MS/MS runs. (B) Phosphoproteome differential analysis. The plot shows the intensity ratio and the p-value of the identified phosphopeptides (n = 7524). 305 and 165 phosphopeptides showed significant down- and up-regulation, respectively (highlighted in blue/red: S0 = 0.05 and FDR = 0.01, n = 5). (C) The result of Kinase-Set Enrichment Analysis (KSEA). All identified phosphopeptides (n=7524) were utilized for the analysis. The z-scores of kinases with four and more substrates are shown. A negative score corresponds to a decrease of the kinase activity. The kinases with |z-score| > 1 are colored blue/red.

For TOC only

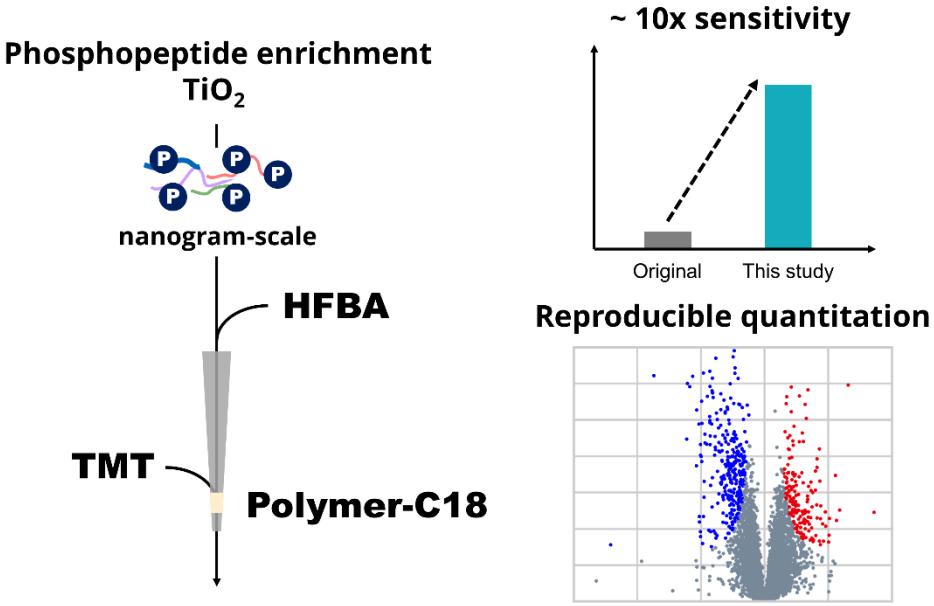
Phosphopeptide enrichment
TiO_2
nanogram-scale
HFBA
TMT
Polymer-C18
~ 10x sensitivity
Original
This study
Reproducible quantitation

Figure 1

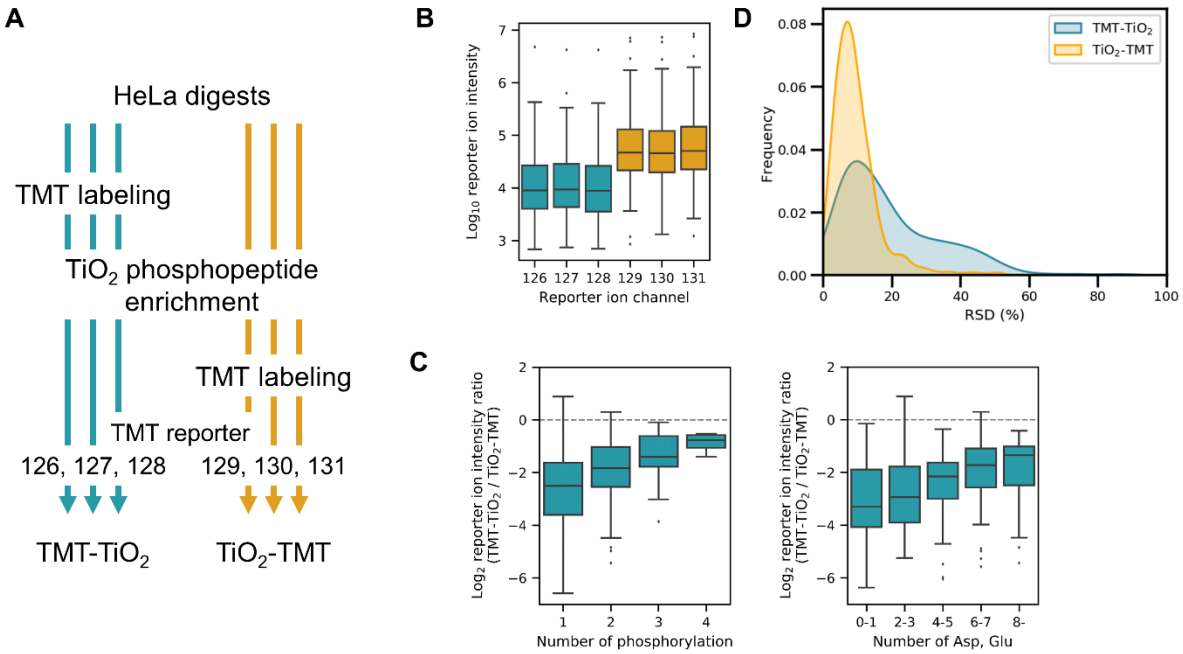
A
HeLa digests
TMT labeling
TiO2 phosphopeptide enrichment
TMT labeling
TMT reporter
126, 127, 128
129, 130, 131
TMT-TiO2
TiO2-TMT
B
Log10 reporter ion intensity
Reporter ion channel
C
Log2 reporter ion intensity ratio (TMT-TiO2 / TiO2-TMT)
Number of phosphorylation
Number of Asp, Glu
D
Frequency
RSD (%)
TMT-TiO2
TiO2-TMT

Figure 2

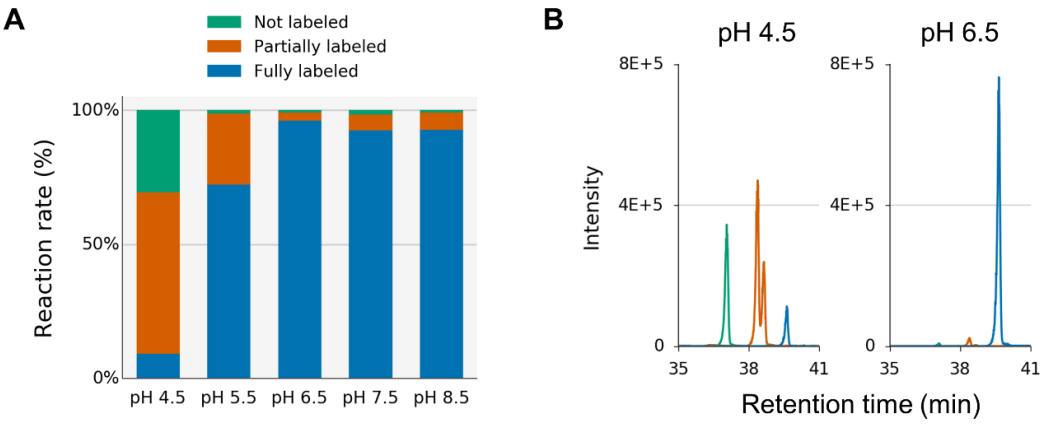
A
Not labeled
Partially labeled
Fully labeled
Reaction rate (%)
100%
50%
0%
pH 4.5
pH 5.5
pH 6.5
pH 7.5
pH 8.5
B
pH 4.5
pH 6.5
8E+5
4E+5
0
Intensity
35
38
41
Retention time (min)

Figure 3

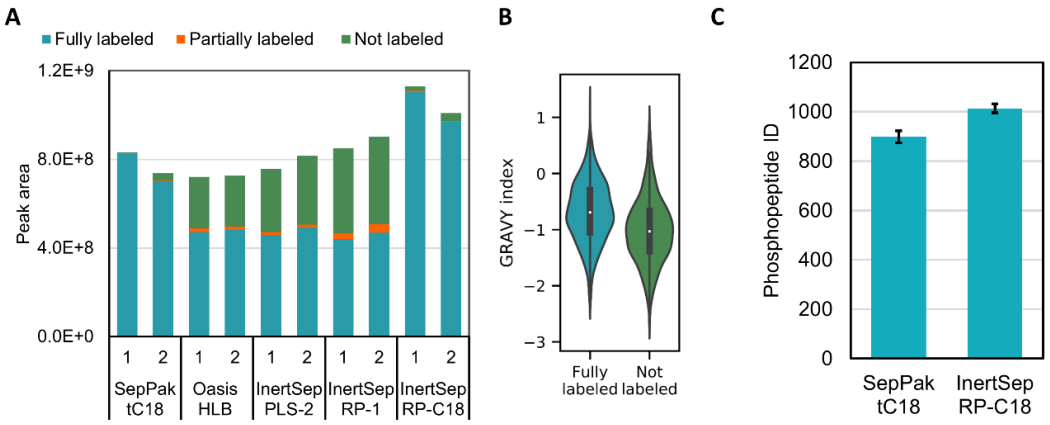
A
Fully labeled
Partially labeled
Not labeled
1.2E+9
8.0E+8
4.0E+8
0.0E+0
Peak area
1 2
SepPak tC18
1 2
Oasis HLB
1 2
InertSep PLS-2
1 2
InertSep RP-1
1 2
InertSep RP-C18
B
GRAVY index
1
0
−1
−2
−3
Fully labeled
Not labeled
C
Phosphopeptide ID
1200
1000
800
600
400
200
0
SepPak tC18
InertSep RP-C18

Figure 4

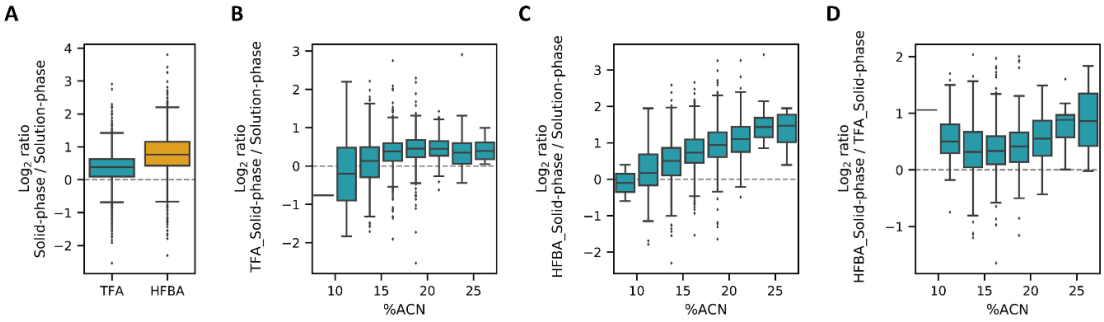
A
B
C
D
Log2 ratio
Solid-phase / Solution-phase
TFA
HFBA
TFA_Solid-phase / Solution-phase
HFBA_Solid-phase / Solution-phase
HFBA_Solid-phase / TFA_Solid-phase
%ACN

Figure 5

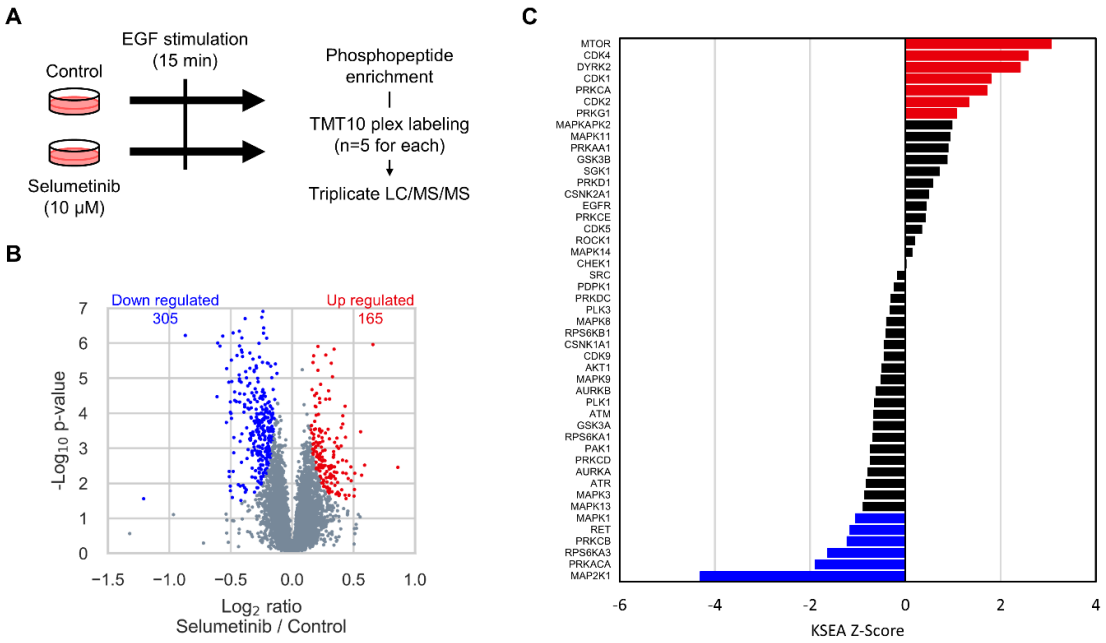
A
EGF stimulation
(15 min)
Control
Selumetinib
(10 μM)
Phosphopeptide
enrichment
TMT10 plex labeling
(n=5 for each)
Triplicate LC/MS/MS
B
Down regulated
305
Up regulated
165
-Log10 p-value
Log2 ratio
Selumetinib / Control
C
MTOR
CDK4
DYRK2
CDK1
PRKCA
CDK2
PRKG1
MAPKAPK2
MAPK11
PRKAA1
GSK3B
SGK1
PRKD1
CSNK2A1
EGFR
PRKCE
CDK5
ROCK1
MAPK14
CHEK1
SRC
PDPK1
PRKDC
PLK3
MAPK8
RPS6KB1
CSNK1A1
CDK9
AKT1
MAPK9
AURKB
PLK1
ATM
GSK3A
RPS6KA1
PAK1
PRKCD
AURKA
ATR
MAPK3
MAPK13
MAPK1
RET
PRKCB
RPS6KA3
PRKACA
MAP2K1
KSEA Z-Score

For TOC only

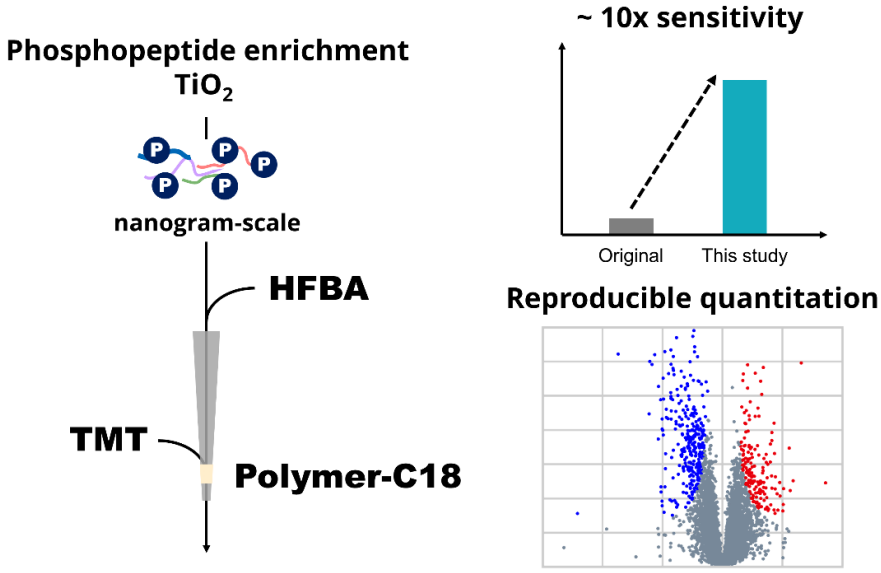
Phosphopeptide enrichment
TiO_2
nanogram-scale
HFBA
TMT
Polymer-C18
~ 10x sensitivity
Original
This study
Reproducible quantitation

Supporting Information

Nano-scale solid-phase isobaric labeling for multiplexed quantitative phosphoproteomics

Kosuke Ogata[1], Chia-Feng Tsai[1], Yasushi Ishihama[1,2,*]

1) Department of Molecular & Cellular BioAnalysis, Graduate School of Pharmaceutical Sciences, Kyoto University, Kyoto 606–8501, Japan

2) Laboratory of Clinical and Analytical Chemistry, National Institute of Biomedical Innovation, Health and Nutrition, Ibaraki, Osaka, 567-0085, Japan.

*Corresponding author:

Tel: +81-75-753-4555, Fax: +81-75-753-4601, E-mail: yishiham@pharm.kyoto-u.ac.jp

---

Table of content

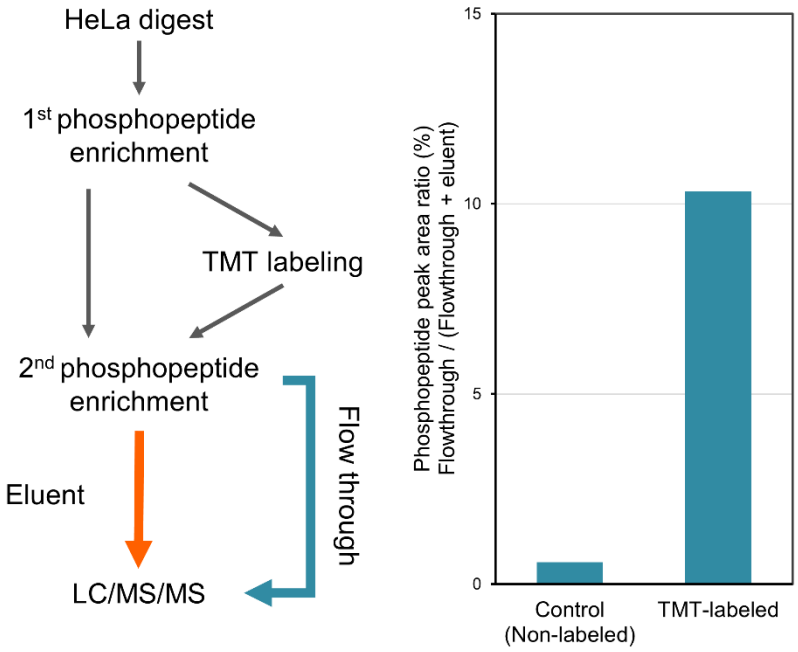

Figure S1. Recovery of TMT-labeled phosphopeptides in TiO_2-based phosphopeptide enrichment.

Analysis of the flow-through fraction from TiO_2-based phosphopeptide enrichment. Tandem phosphopeptide enrichment experiments were performed to analyze phosphopeptides in the flow-through fraction. The peak areas of identified phosphopeptides were compared between eluted and flow-through fractions.

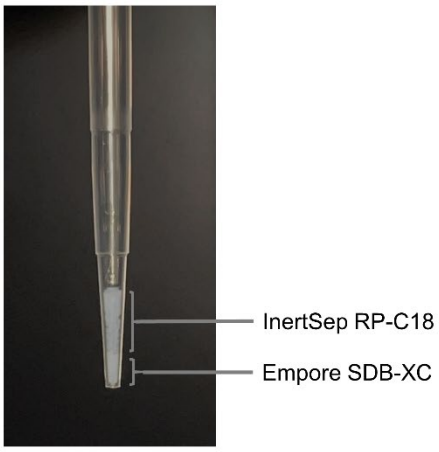

Figure S2. Photograph of a StageTip used for solid-phase TMT labeling.

A

		126	127N	127C	128N	128C	129N	129C	130N	130C	131
Peptide amounts before TiO_2 enrichment (µg)	amount applied to tipTMT labeling	1	1	5	5	10	10	50	50	100	100
	amount injected to LC/MS/MS	1	1	5	5	10	10	10	10	10	10

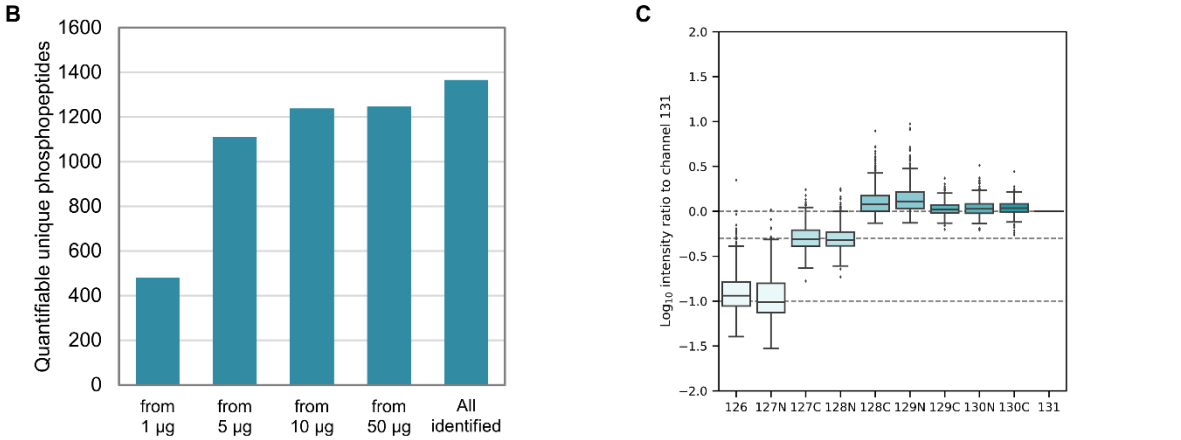

Figure S3. Applicable range of peptide amounts in the optimized solid-phase TMT labeling method. Phosphopeptides were enriched by TiO_2 chromatography from HeLa digests, and were divided into the amounts indicated in (A). After labeling with TMT10plex reagents by the optimized solid-phase TMT labeling method. The indicated amounts of peptides were mixed and analyzed by LC/MS/MS. An Orbitrap Exploris 480 mass spectrometer equipped with FAIMS pro and an UltiMate 3000 RSLCnano pump (Thermo Fisher Scientific) was employed for the analysis. (B) The bar chart shows the number of quantifiable phosphopeptides. Phosphopeptides from 1 µg with peaks detected in all ten reporter ion channels were considered as quantifiable. Phosphopeptides from 5 µg, 10 µg, and 50 µg with eight reporter ions (127C, 128N, 128C, 129N, 129C, 130N, 130C, and 131), six reporter ions (128C, 129N, 129C, 130N, 130C, and 131), and four reporter ions (129C, 130N,130C, and 131), respectively were considered quantifiable. (C) The box plot shows the upper quartile, median, and lower quartile for the TMT reporter ion intensity ratios to channel 131. Outliers were identified using box-plot statistics (threshold: 1.5 x the interquartile range (IQR)). Dashed lines represent expected ratios. The phosphopeptides quantifiable from 1 µg were plotted.

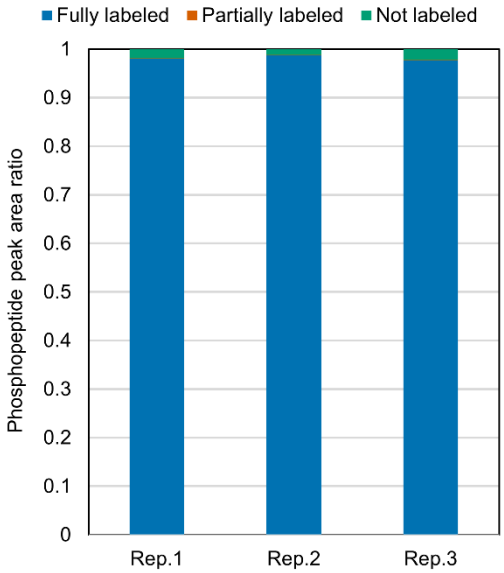

Figure S4. Labeling efficiency of solid-phase TMTpro labeling.

The bar graph showed the peak area ratio of TMTpro-labeled phosphopeptides from HeLa cell digests using the optimized solid-phase TMT labeling protocol. The samples were prepared in triplicate. The peptide was categorized into three classes according to the number of TMT-tags. Not labeled: The peptide with no TMT-tag. Partially labeled: The peptide with a TMT-tag but either the lysine side chain or peptide N-terminus is not labeled. Fully labeled: The peptide completely labeled with TMT. Over 98% of the phosphopeptide peak area was due to fully labeled peptides.

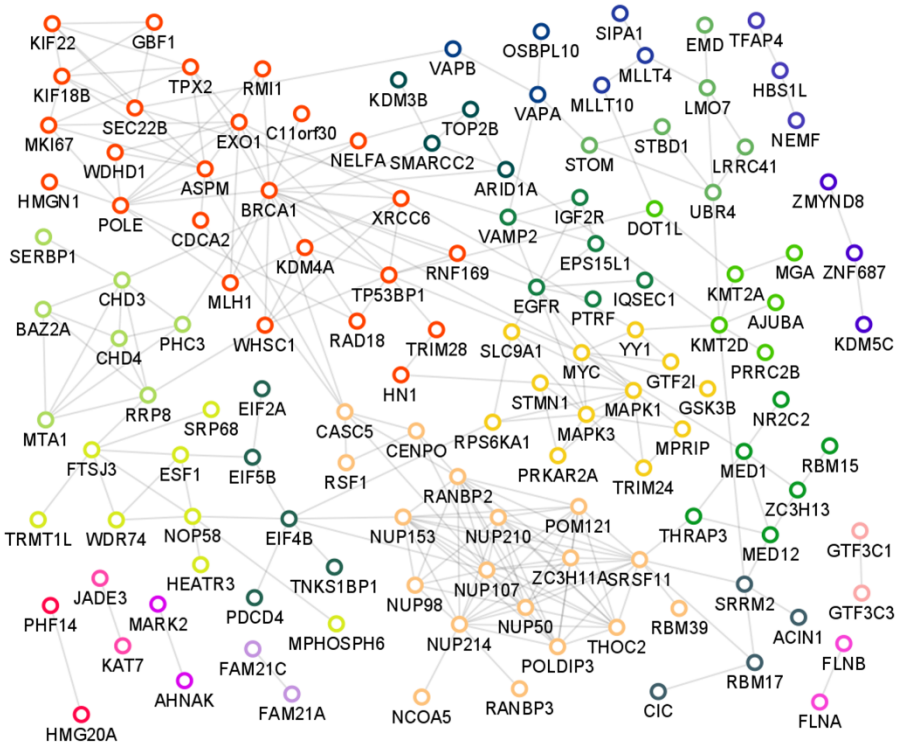

Figure S5. STRING network analysis of proteins having decreased phosphopeptides upon selumetinib treatment.

STRING network (v11.0) of high-confidence interactions (minimum confidence score of 0.700) among proteins with decreased phosphosites upon selumetinib treatment. Colors on nodes indicate the clusters based on STRING MCL clustering (inflation parameter: 1.6). Disconnected nodes are not shown.